

EXPERIMENTAL AND NUMERICAL STUDIES ON INITIAL STAGES OF SAGD PROCESS FOR HEAVY OIL RECOVERY

K. SASAKI & S. AKIBAYASHI
Akita University - Japan

N. YAZAWA & N. KUMAGAI
Japan National Oil Corporation - Japan

Abstract

Experiments and numerical simulations on initial stages of the steam-assisted gravity drainage (SAGD) process were carried out using two-dimensional scaled reservoir models in order to investigate oil production mechanism and performance. The rising or growing process of the initial steam chamber was visualized using video and thermal-video pictures. For the case of conventional SAGD, oil production rate increased with increasing vertical well spacing; however, the lead-time for the gravity drainage to initiate oil production became longer. The results suggest that the well spacing can be used as a governing factor to evaluate oil production rate and lead-time in the initial stage of the SAGD process.

Furthermore, micro-phenomena at the inclined interface of the steam chamber with high-resolution optical-fiber scope were visualized. The fine water droplets approximately 0.02 mm in diameter were observed at the interface between steam and oil phases. The behavior was seemed that the droplets diffuse into heated oil and then create water-in-oil emulsion. The water droplets with same range of size were also observed in the produced emulsion.

The numerical simulation using the STARSTM was also performed to carry out history-matching with the experimental results for the conventional SAGD process. The simulation uses a two-component (water and heavy oil) black oil, three-phase (water, heavy oil and steam) and three-dimensional numerical model. The results from the history-matched numerical simulation are found to be in reasonable agreement with those of the experiment for oil production rate, cumulative oil production, steam chamber shape and temperature contours in the initial stages to create the steam chamber.

Based on these results, it was found that the instability over the steam chamber is not enough to recover the upper regime of the oil seam after the initial stage. The modified SAGD process by adding intermittent steam stimulation from the lower well (named SAGD-ISSLW) has been proposed to enhance the oil production from the upper regime.

INTRODUCTION

It is not easy to produce heavy oil efficiently and economically. However, as shown in the reports of the UTF projects (phase A and B) in Canada, the steam assisted gravity drainage, SAGD, process has proven to be very superior process for the recovery of the bitumen due to its high recovery factor^{9), 16)}. Butler and his co-workers have developed the process¹⁾⁻⁸⁾. Their ideas was to overcome the problems associated with the highly viscous bitumen by gravity drainage in steam chambers generated by displacement of heavy oil (Fig. 1).

Recently, the surface-drilled SAGD process has been tested as more economical one at UTF. The Japan Canada Oil Sands Limited (JACOS) has also successfully drilled seven horizontal pairs

from the surface for bitumen production at Hangingstone, Athabasca. The SAGD process operated by steam injection from upper well and production from lower well like that of UTF project, is hereinafter referred as “Conventional SAGD.”

A recent problem focused on is that growing up to the regime over the steam chamber is slower than simulated results using Butler theory. Another problem of the conventional SAGD process is lead-time required generating a steam chamber in near break-through condition between two wells before the rising chamber stage. A modified process to enhance the growing rate of the steam chamber by forming stronger fingering should be the more economical SAGD process.

In this study, expanding or rising process of steam chamber and drainage mechanism along the chamber interface at the initial stage have been investigated by video-pictures and temperature distributions visualized using thermal-video system. Furthermore we observed microscopic phenomena using fiberscope system inserted at the steam chamber boundary in order to investigate the emulsion behavior in the steam chamber.

EXPERIMENTAL APPARATUS AND PROCEDURES

Experiments were performed in scaled two-dimensional reservoir models with porous packing materials to investigate and visualize steam chamber behavior and oil production mechanisms with respect to heat and mass transfer phenomena. Figure 2 shows the schematic figure of the experimental apparatus. The apparatus consisted of a water pump, steam generator, steam accumulator, two-dimensional scaled reservoir model, production control mechanism, visualization system, and the measurement and data acquisition system using a data logger and a computer. The scaled physical reservoir models (200×200 mm and 300×300mm, thickness = 4.5 or 9.6 mm) with tightly packed glass-beads (diameter = 0.18-0.25mm, porosity = 38%, permeability = 115×10^{-12} m²) were used. For each test, the model was saturated with heavy-oil (molecular weight=490g/g-mole, density = 998kg/m³, viscosity = 0.12Pa·s at 106 °C) using a vacuum pump. In most experiments, the vertical well spacing was set as $L = 100$ mm, and dry steam of 106 °C was injected under the constant steam pressure of 20kPa to suppress the pushing effect by steam. In the experiment, steam was trapped at the production well, to prevent its escape at the time of breakthrough, by a controlling valve which was set to be automatically closed at a rate of about 90 % when temperature of the production fluid reached 95 °C. After near break-through between two wells, oil production was controlled successfully to keep the temperature of production fluids mixture (oil and condensate) under the set temperature of 95 °C. The rates of oil production and expanding area of the steam chamber were measured and analyzed. Furthermore, temperature distributions using infrared thermal video system were compared with visualized video-pictures. The fiberscope 2mm in diameter consists of 30,000 glass fibers was installed at the position 75 mm over and 38 mm right from the production well. The boundary of the steam chamber passes its position during $t = 3-4$ hours. The range of the dimensionless factor, B_3 , defined by Butler (1985) is between 7.6 and 10.4, which is relatively close to the JACOS field value estimated between 4.5 and 9.2(Sasaki, et al., 1999).

We did not employ pre-heating in the present experiments, because pre-heating would interact with the well structure and materials, heating not only the reservoir but also both side plates of the two-dimensional models. The heat losses from the reservoir models have been estimated as 60 to 75 % of total injected heat for the amount of condensed water flowed down on the transparent acrylic-plates.

EXPERIMENTAL RESULTS

Visualized Pictures

One of the series of visualized pictures of the steam chamber by the conventional SAGD process is shown in Fig. 3. The chamber shape after break-through is more like an “egg,” which is different from the triangle-like shape obtained by Butler and Stephen¹³. The angle subtended at the chamber bottom near the production well is 68-73 °, relatively larger than the 64° reported in Butler and Stephen¹³. A typical picture showing temperature distribution recorded by the thermal-video system is shown in Fig. 4, with the boundaries of the steam chamber and fingering region and three isotherm lines. The temperature at the interface of the steam chamber is almost coincident with a contour line (80 °C) in the upper region over the injection well for the conditions of the present experiment (conventional SAGD, pressure difference; $\Delta p = 20$ kPa, steam temperature; $T_s = 106$ °C). However, the interface temperature in the lower region is higher than 80 °C. Furthermore, the layer between the 80 °C isothermal line and chamber interface becomes thicker near the production well, because the region near the production well has no gravity flow-down and stores heat.

Production Fluids Mixture

Production fluids consisted of single-phase condensate (water) and water-in-oil emulsion phase after break-through. Single-phase heavy oil was produced only at the initial time after starting steam injection. The emulsion was produced as water-in-oil (water droplets 0.01- 0.07 mm in diameter) as shown in Fig. 6. The size of droplets is 10^{-1} order of the glass beads used in the experiments. Water gained from breaking the emulsion shows net steam used for heating and recover heavy oil. Figure 6 shows a typical result for the emulsified water/oil volume ratio. Before the start of the rising chamber, the ratio was less than 1.0. However, it became almost flat at 1.2 ± 0.3 after break-through time. This value may show the net steam/oil ratio (SOR) in our experiments. The oil volume fraction of emulsion produced after break-through time was approximately 45 %. Viscosity of the emulsion is almost twice of single phase of oil for the steam saturated temperature.

We observed the boundary region between steam and oil phases on the steam chamber interface using the glass fiberscope. Figure 7 shows four video pictures on different times. The very fine water droplets produced at the steam-oil boundary were involved in oil, and then it may produce the water-in-oil emulsion. In addition, the boundary between two phases moved to right direction with recovering oil or expanding of the steam chamber.

Effect of Vertical Well Spacing

The production from the rising steam chamber was sensitive to the location of the steam-injection well. The position of the upper well was varied, while the production wells were fixed near the bottom of the reservoir. Figure 5 shows the oil production rate of the conventional SAGD process against the five different vertical spacing between the two well centers, L . On the basis of the experimental results, a similarity of production rate for different vertical spacing has been investigated. The oil production rate increases with increasing vertical well spacing between two wells, but the lead-time to start oil production by gravity drainage becomes longer. It is assumed that larger chamber may be created by the effects of steam convection when the injection well is moved to the upper area. The maximum oil production rate is defined as q_{pmax} , which was recorded near the break-through time. The break-through time, t_{BT} , increases with increasing vertical well spacing, L , approximated as $t_{BT} \propto L^{1/2}$. Furthermore, based on the similarity of the production curves, the production rate, q , is expressed as $q \propto L^{1/2}$. Thus, L can be used as a governing factor to evaluate production rate and lead-time in the initial stage of the conventional SAGD process. Butler et al.¹³⁾⁻¹⁵⁾ reported similar performance based on the reservoir thickness; their work focused on the expansion of the chamber after arriving at the overburden.

Production Behavior at Steam Chamber Interface

The upper regime of the model reservoir was not fully recovered after 20 hours in the present experiment; thus the gravitational instability of the upper regime over the steam chamber was not effective to recover it. It is assumed that a kind of barrier, such as emulsion layer with much high viscosity than the residual oil, was generated at the upper boundary between steam and oil phases. On the other hand, the horizontal growing mechanism of the steam chamber after break-through is basically caused by gravitational force according to the SAGD theory. However, authors assume that friction force and convective heat transfer on the heated oil generated by steam convection flow moves downward gives additional production mechanism.

NUMERICAL MODELLING

The simulation uses a two-component (water and heavy oil) black oil, three-phase (water, heavy oil and steam) and three-dimensional numerical model. Considering the necessity of sufficiently fine grids for accurate evaluation of a rising steam chamber spreading sideways and upwards, a grid sensitivity study was conducted in order to determine the appropriate vertical and horizontal lengths of grid blocks. Several numerical runs, with varying grid sizes, led to a selection of (15×3×15) configuration to provide sufficient accuracy of results. Figure 8 shows the configuration of the grid blocks with their numbers and respective sizes, and location of the wells. Rock and heavy oil properties, initial conditions, and saturation endpoints are same as those in the experiment, most of which are measured values (see Sasaki et al.¹⁸).

Convective heat transfer model in the simulator is used to evaluate the experimental heat loss from the model (siding acrylic resin plates, with a heat conductivity of $\lambda=0.13$ J/cm·min°C) to the surroundings air. The overall convective heat transfer coefficient was given as $\alpha = 0.041$ J/cm²min°C and was input for each of the grid blocks of the resin plates.

Two horizontal wells are assigned, and the discretized wellbore model is used to put into effect the transient flow behavior at the wellbore of the injector. Horizontal producer is assigned into the grid blocks. A starting operating bottomhole pressure (BHP) of 101.3 kPa (atmospheric) and a minimum BHP of the same value are set. The action is taken to prevent escape of excessive steam at the time of breakthrough. These conditions are same as those in the experiment. Horizontal injector is in the same manner, $L = 100$ mm above the production well.

In the experiment, the BHP was almost constant at a value of 121.6 kPa. But, due to the history matching, the operating constraint is set to be the steam injection rate (in terms of cold water equivalent, CWE) which is then altered, based on the experimental data, at the beginning of each of 10 min-periods.

In this numerical simulation study, several numerical runs were conducted with both linear and non-linear two-phase relative permeability functions, with zero and non-zero end-point saturations, to investigate their effects on results. It was noted that shape of the rising steam chamber and cumulative oil production are affected by the relative permeability functions employed. The numerical simulations using linear relative permeability functions with non-zero end-point saturations provided good agreement of the steam chamber shape to the experimental observations, while the linear functions as well as non-linear functions did not. Thus, the linear relative permeability functions with non-zero end-point saturations were used for the history matching calculations. The steam chamber apparently disagrees with the conclusion drawn by Chow and Butler⁸, which might possibly be attributed to the large difference in the average permeability values of the two studies.

In the numerical model, steam trapping is provided by an operating constraint with a value of

differential temperature of 5 °C lower than the saturated steam temperature. The bottom-hole pressure of the well is kept high enough that live steam does not appear in the well block, very similar to that in the experiment.

NUMERICAL HISTORY MATCHING RESULTS

In order to get good history-matched results, the injected steam quantity based on the experimental data is input at each data point for the entire period of the experimental time (each of 10 min intervals) for the entire period of the experimental time. Figure 9 compares the numerical oil production rate with the experimental rate. The numerical oil production rate increases with time and attains a maximum rate at 160 min, which is the time just before the steam breakthrough. The steam breakthrough of the conventional SAGD process was noted at 170 min in the experiment. Then, a steady decrease in the oil production rate is observed because of the reservoir depletion. The numerical result resembles, in slopes and the shapes, the experimental oil production rate. Figure 10 shows the experimental cumulative steam injection at varying times. The overall cumulative amount is 548 cc at the simulation time $t = 550$ min.

The experimental cumulative oil production was compared with that for the numerical simulation. The numerical result at $t = 550$ min reported a cumulative amount of 49 cm³, which is less than the experimental volume of 64 cm³. The slopes of the cumulative oil production curves match satisfactorily. Obviously, the numerical cumulative oil production curve during 40-180 min extends ahead of the experimental one. The numerical curve, then, lags behind the experimental value. It is during this period that the maximum degree of emulsification is found and the oil produced was as water-in-oil emulsion in the experimental studies. Furthermore, for the case of the simulation model, the upper regime of the reservoir was completely recovered until $t = 1200$ min after steam injection, which is much different from the experimental ones. It seems to be caused by somewhat incomplete representation of transient flow behavior and instability in the numerical simulator.

With the selection made for the relative permeability functions to be used in the numerical simulation, a satisfactory agreement was obtained between the shapes of the experimental and the numerical. It was noted that the simulator can model steam rise and steam chamber growing sideways and upward. Both experimental and numerical steam chambers were observed to be growing at similar rates during initial stage. Figure 11 compares the numerical and the experimental steam chambers with temperature contours at $t = 550$ min.

SAGD-ISSLW METHOD

A modified SAGD process named SAGD-ISSLW¹²⁾ has been proposed to enhance oil production rate after the steam break-through between two wells. The process uses the lower horizontal well with the dual functions of intermittent steam stimulation and continuous oil-production rather than for oil production only. Meanwhile, the steam is also injected continuously through the upper well like the conventional one. From the results of the experiments for the new process, the lead time to generate near break-through condition between two wells was shortened 20 %, and oil production rate was enhanced 16 % compared to that of conventional SAGD process at $t = 540$ min (see Figures 12 and 13). The expanding rate of the chamber area including fingering area is enhanced 43 % compared to the conventional SAGD process. Expanding rates of chamber area upward and horizontal directions were larger than the conventional one. It is assumed that the intermittent steam injection from the producer enhanced steam convection effect on the side interfaces and instability at the upper interface of the steam chamber. Especially, the instability causes larger fingering in the upper area, and enhances the chamber growing upward by controlling the steam flow direction from the upper well using the injection steam from the lower well.

CONCLUSIONS

Experiments on the SAGD process were carried out using two-dimensional scaled and visual reservoir models. The expanding or rising process of the steam chamber and the drainage mechanism along the steam chamber interface were investigated using video-pictures and temperature distributions visualized using a thermal-video system. The rates of oil production and the expanding area of the steam chamber at the initial stage were measured and analyzed. The similarity of production rate for different vertical spacing between two wells was also investigated. The net steam/oil ratio (SOR) has been evaluated as 1.2 ± 0.3 , based on the emulsified water/oil volume ratio. In addition, the micro-scopic formation of emulsion was observed using the fiberscope inserted at the steam chamber boundary. The fine water droplets produced at the steam-oil boundary moved into oil phase, then produced the water-in-oil emulsion. In addition, it was found that the gravitational instability of the upper regime over the steam chamber was not enough to recover the upper regime by somewhat barrier between steam and oil near the top boundary of the steam chamber.

The STARSTM was used in order to simulate the present experimental data for the conventional SAGD process. The numerical results for the initial stage are found to be in reasonable agreement with those of the experiment, for oil production rate, cumulative oil production, the steam chamber and temperature contours in the model. Varying physical conditions (steam injection pressure, vertical separation between injection and production wells, and reservoir thickness) are found to have similar effects on the performance of the SAGD process both in the experimental and numerical studies for the initial stage. On the other hand, the simulation results, that the upper regime is fully recovered after the initial stage, are different from the experimental ones.

The SAGD-ISSLW proposed as an enhanced and economical SAGD process uses a production well with the dual functions of intermittent steam stimulation and continuous oil production, similar to the single SAGD well, instead of the conventional production well. In the SAGD-ISSLW process, adding intermittent steam injection from the lower well while steam injects continuously from the upper well shortens the time to generate near break-through condition between the two wells. The intermittent steam stimulation from the producer accelerated instability of the interface near the ceiling by forming larger fingering into the upper regime. It enhanced the oil production rate compared with that of conventional SAGD process. The steam may be injected earlier due to the quick generation of the steam chamber around the lower well, thus pre-heating of reservoir around the wells can be shortened and it will help set longer vertical spacing between the two wells. Furthermore, it will be easier to control expanding rate of the steam chamber after break-through by changing rate and interval of the intermittent steam injection from the lower well.

We expect that the SAGD-ISSLW process is likely to prove its effectiveness in heavy oil recovery using the SAGD process. Experiments and simulation with CMG STARSTM are underway in consideration of emulsion formation at the steam chamber boundary.

Acknowledgements

This study has been supported by the Technical Research Center of the Japan National Oil Company. We would like to thank Dr. Q. Doan (Univ. of Alberta), Dr. S.M. Farouq Ali (Univ. of Alberta), Dr. H.K. Sarma (JNOC) and Mr. K. Ohno (JNOC) for their helpful advice.

References

1. Butler, R.M.: "A New Approach to the Modeling of Steam-Assisted Gravity Drainage," *JCPT*, 24-3 (1985), 42-52

2. Butler, R.M.: *Thermal Recovery of Oil & Bitumen*, Prentice Hall Inc., New Jersey (1991), 285-359
3. Edmonds, N.R., Gittins S.D., Kovalsky, J.A. and Pennachioli, E.D.: "Review of Phase A Steam-Assisted Gravity-Drainage Test," *SPE Reservoir Eng.*, 9-2 (1994), 119-124
4. O'Rourke, J.C., Chambers, J.I., Sugget, J.C. and Good, W.K.: "UTF Project Status and Commercial Potential," paper Petroleum Soc. of CIM and AOSTRA, 94-40 (1994), 5
5. Chung, K.H.: "Heavy Oil Recovery by The Steam Assisted Gravity Drainage Process," Ph.D. Thesis, University of Calgary (1988)
6. Chung, K.H. and Butler, R.M.: "Geometrical Effect of Steam Injection on the Formation of Emulsions in The Steam-Assisted Gravity Drainage Process," *JCPT*, January-February (1988), 36-42
7. Chung, K.H. and Butler, R.M.: "A Theoretical and Experimental Study of Steam Assisted Gravity Drainage Process," Meyers and Wiggings Eds., *Proc.*, The 4th UNITAR/UNDP Int. Conf. on Heavy Crude and Tar Sands, Vol. 4, AOSTRA, Edmonton (1989), 191-210
8. Chow, L. and Butler, R.M.: "Numerical Simulation of the Steam-assisted Gravity Drainage Process," paper Petroleum Soc. of CIM and AOSTRA 94-63 (1994)
9. Mukherjee, N.J. et al.: "A Comparison on Field Versus Forecast Performance for Phase B of the UTF SAGD Project in the Athabasca Oil Sands," *Proc.*, UNITAR, Int. Conf. on Heavy Crude and Tar Sands, Houston (1995), 581-595
10. Butler, R.M.: "Steam Assisted Gravity Drainage: Concept, Development, Performance and Future," *JCPT*, February (1994), 44-50
11. Liederth, D.: "ELAN Showing Positive Single-Well SAGD Results," *Daily Oil Bulletin*, May 2 (1995)
12. Sasaki, K. et al.: "A New Concept of Enhanced SAGD Process by Adding Intermittent Steam-Stimulation on Lower Horizontal Production-Well(SAGD-ISSLW)", *Proc. of 15th World Petroleum Congress(Beijing)*, Vol.2(Exploration, Production and Downstream), John Wiley & Sons, pp.511-513 (1998)
13. Butler, R.M. and Stephens, D. J. : "The Gravity Drainage of Steam-Heated Heavy Oil to Parallel Horizontal Wells," *JCPT*, April-June (1981), 90-96
14. Butler, R.M.: "Rise of Interfering Steam Chambers," *JCPT*, 26-3 (1987), 70-75
15. Sugianto, S. and Butler, R.M.: "The Production of Conventional Heavy Oil Reservoirs with Bottom Water Using Steam-Assisted Gravity Drainage," paper The Petroleum Soc. of CIM, 89-40-33 (1990)
16. Komery, D.P., Luhning, R.W. and O'Rourke, J.C.: "Towards Commercialization of UTF Project Using Surface Drilled Horizontal SAGD Wells," paper The Petroleum Soc. of CIM, 95-60 (1995)
17. Gooble, L.M.A. and Good, W.K.: "Shell/Alberta Department of Energy Peace River Horizontal Well Demonstration Project—A Test of The Enhanced Steam Assisted Gravity Drainage Process," paper Petroleum Soc. of CIM and AOSTRA, 94-41 (1994)
18. Sasaki, K. et al.: "Numerical and Experimental Modelling of the Steam-Assisted Gravity Drainage (SAGD) Process", *Proc. of CIM*, CIM Paper 99-21 (1999)
19. Sasaki, K. et al.: "Experimental Modeling of the Steam-Assisted Gravity Drainage Process-Enhancing SAGD Performance with Periodic Stimulation of the Horizontal Producer-", *Proc. of SPE Annual Meeting(Houston)*, SPE 56544 (1999)

SI Metric Conversion Factor

cP ×1.0 E-03 = Pa·s

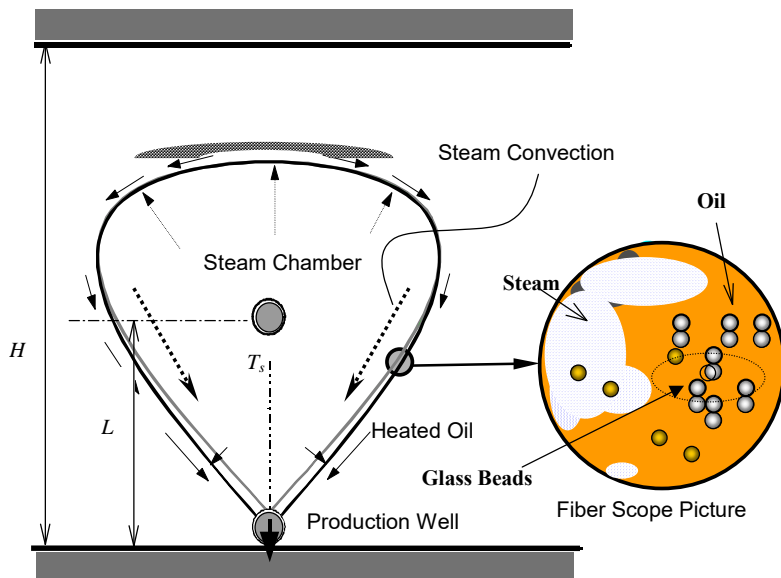


Fig. 1 Definition of Steam Chamber

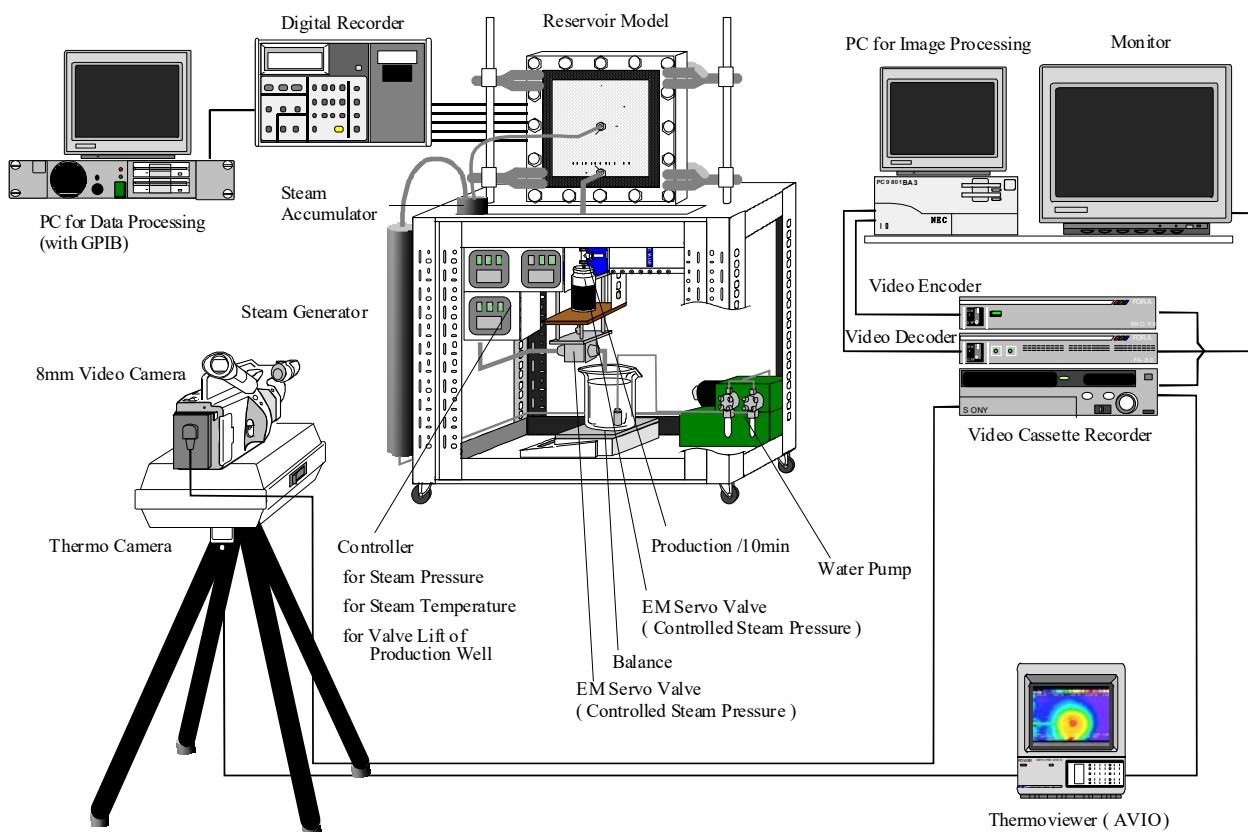


Fig. 2 Experimental Apparatus

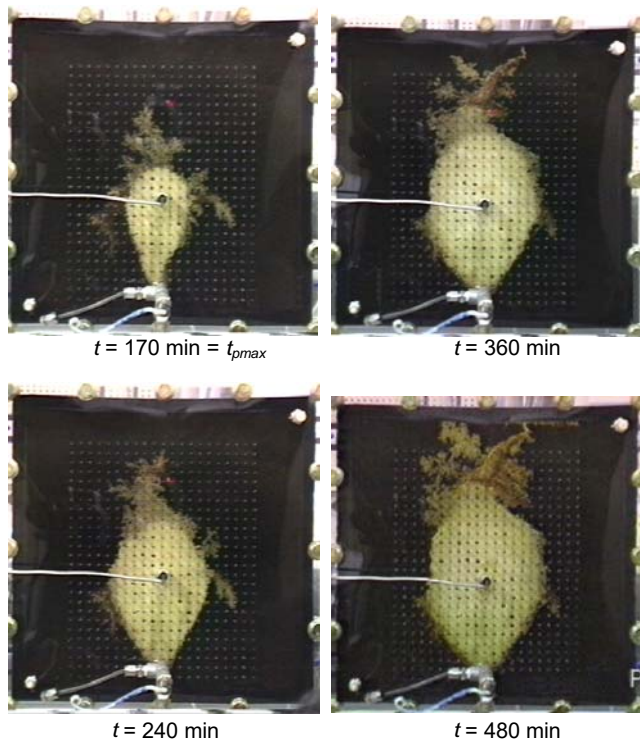


Fig. 3 Visualized Pictures of Growing Rising-Steam Chamber with Time (Conventional SAGD, 300 ×300 mm, 4.5 mm thickness model)

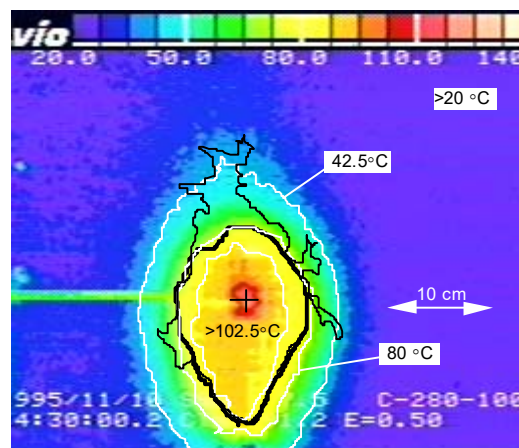


Fig. 4 Temperature Distribution Captured by the Thermal Video System. (Thick black line shows the steam chamber interface and thin one shows the expanding boundary of fingers.) (Conventional SAGD, 300 ×300 mm, 4.5 mm Thickness Model, $t = 240$ min.)

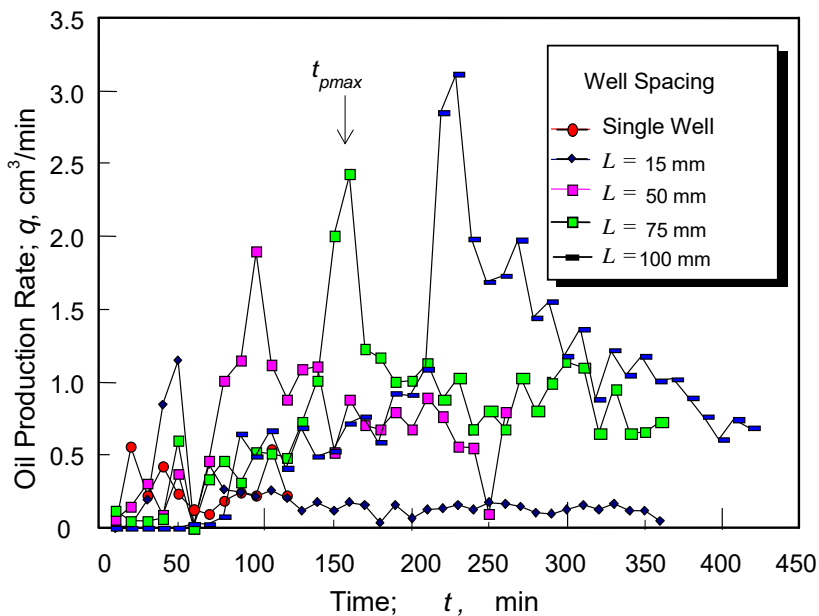
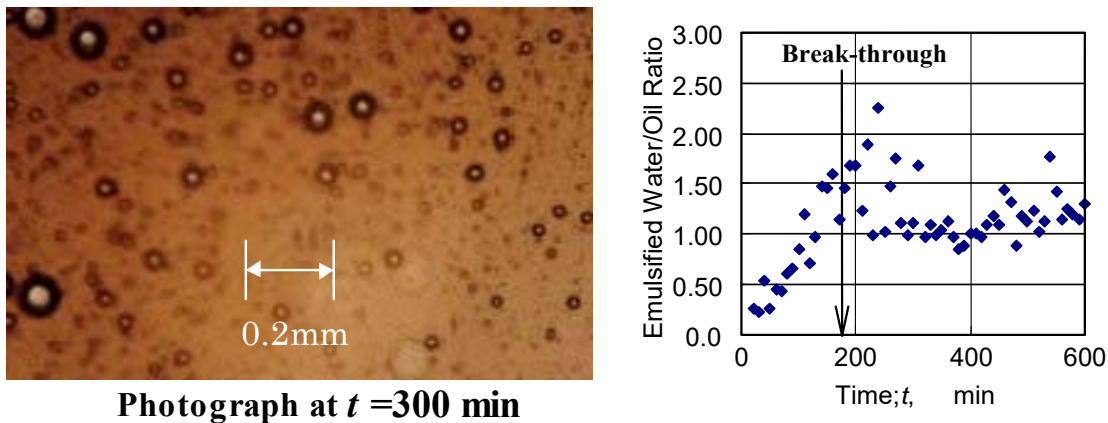


Fig. 5 Effect of Vertical Well Spacing upon Oil Production Rate for Conventional SAGD



Photograph at $t = 300$ min

Fig. 6 Photograph of Emulsified Production Oil and Emulsified Water/Oil Ratio versus Elapsed Time. (Conventional SAGD, 300 ×300 mm, 9.5 mm Thickness Model)

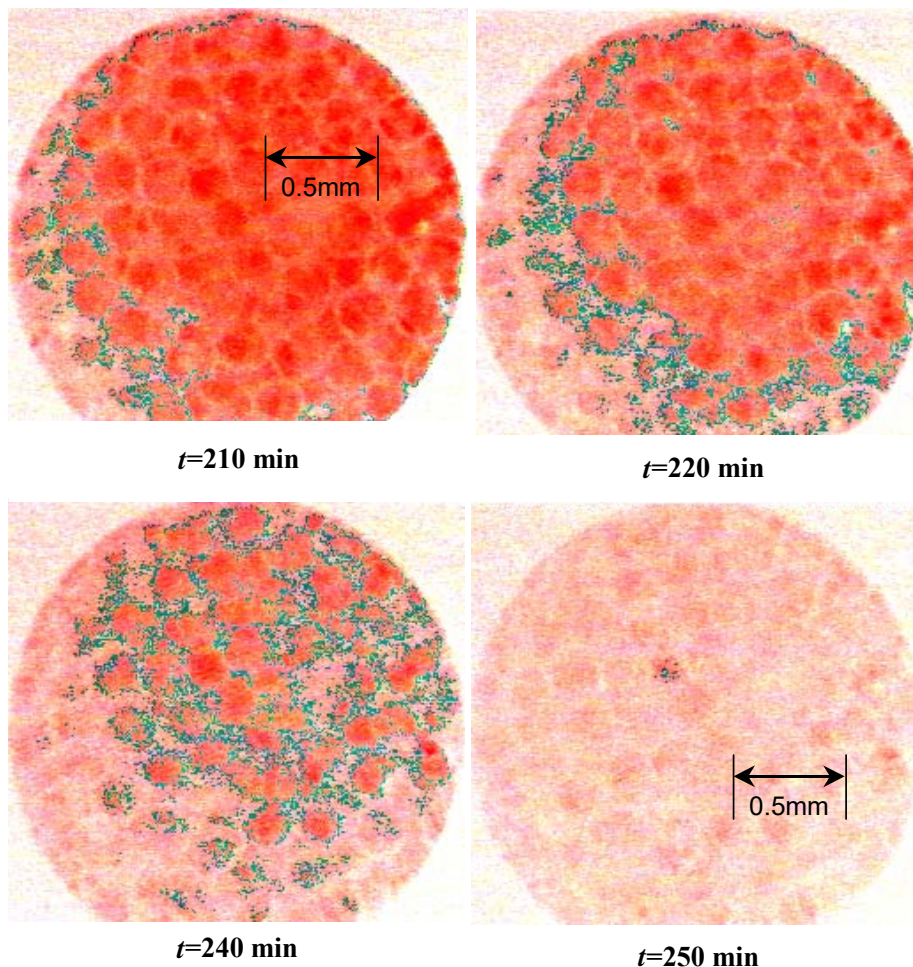


Fig.7 Fiber Scope Visualization Pictures (Left and right sides of the pictures show steam and oil phases respectively. Fine water droplets were observed at the boundary) (Conventional SAGD, $t = 300$ min., 300×300 mm, 9.5 mm Thickness Model)

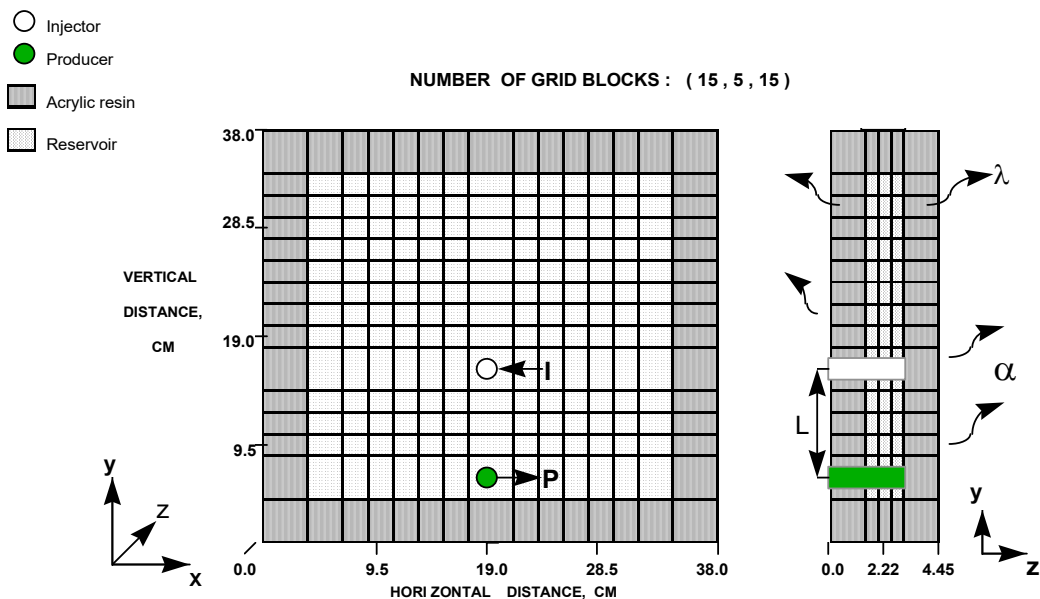


Fig. 8 Grid block Configuration of Numerical Reservoir Model

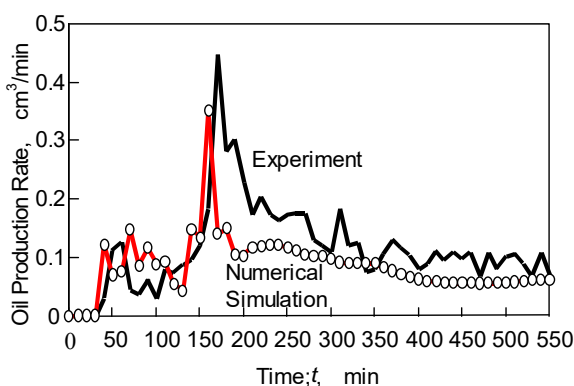


Fig. 9 Comparison of Oil Production Rate vs. Time (Conventional SAGD)

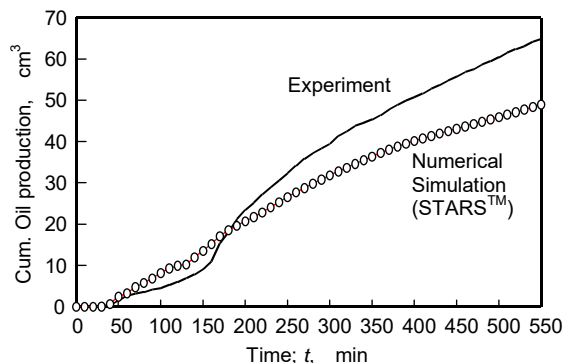


Fig. 10 Comparison of Cumulative Oil Production vs. Time (Conventional SAGD)

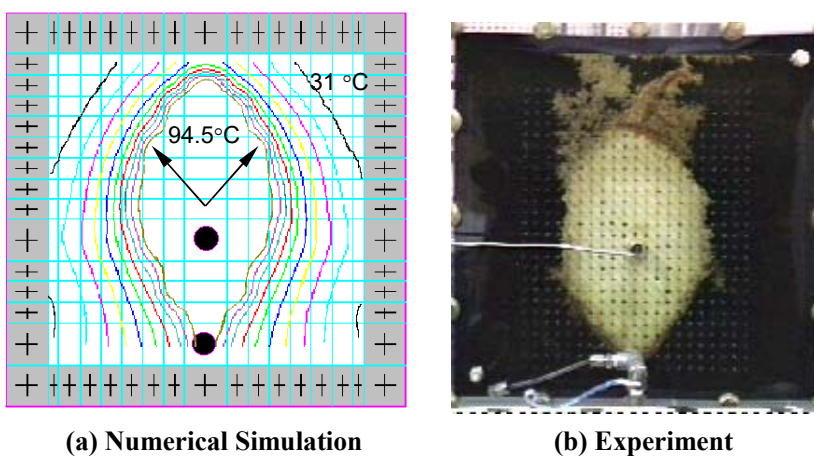


Fig.11 Comparison of Steam Chambers at $t = 550$ min

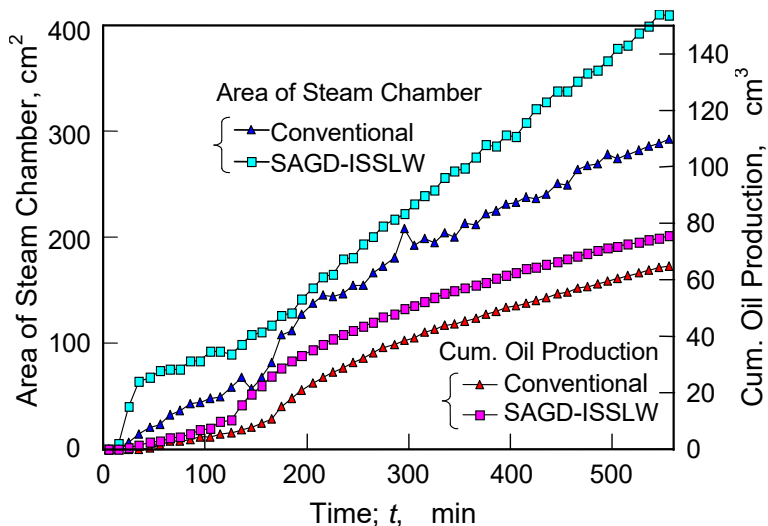


Fig. 12 Comparison Area of Steam Chamber and Cumulative Oil Production between Conventional and SAGD-ISSLW Processes. (300×300 mm, 4.5 mm thickness Model)

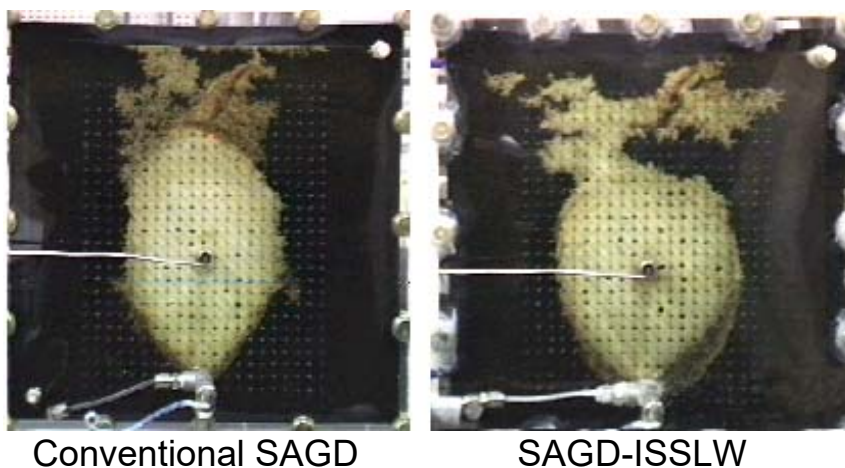


Fig. 13 Comparison of Steam Chamber between Conventional SAGD and SAGD-ISSLW. (300×300 mm, 4.5 mm Thickness Model, $t=540$ min)